Acta Materialia xxx (2015) xxx–xxx

Contents lists available at ScienceDirect

Acta Materialia

journal homepage: www.elsevier.com/locate/actamat

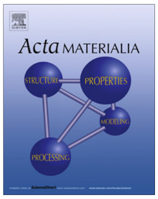

Study of precipitation in Al–Mg–Si alloys by Atom Probe Tomography I. Microstructural changes as a function of ageing temperature

M.W. Zandbergen [a,*], Q. Xu [b], A. Cerezo [a], G.D.W. Smith [a]

[a] Department of Materials, University of Oxford, Parks Road, Oxford OX1 3PH, UK
[b] National Center for HREM, Kavli Institute of Nanoscience, Delft University of Technology, Lorentzweg 1, NL-2628 CJ Delft, The Netherlands

ARTICLE INFO

Article history:
Received 8 December 2014
Revised 10 August 2015
Accepted 11 August 2015
Available online xxxx

Keywords:
Aluminium alloys
Ageing
Atom Probe Tomography
Precipitation
Metastable phases

ABSTRACT

Atom Probe Tomography (APT) analysis and hardness measurements were used to characterise the early stages of precipitation in an Al–0.51 at.%Mg–0.94 at.%Si alloy. The changes in microstructure were investigated after single-stage or multi-stage heat treatments including natural ageing at 298 K (NA), pre-ageing at 353 K (PA), and automobile paint-bake ageing conditions at 453 K (PB). A wide range of particle sizes and compositions was typically present after a given heat treatment. Changes in particle sizes and compositions were found to be continuous, without abrupt changes of chemistry or morphology during the evolution of the initial clusters into GP zones and fine-scale precipitates. No phases were observed which were intermediate between GP zones and β''. NA had a deleterious effect on the PB hardening response, which was caused by a decrease in the rate of formation of stable, elongated precipitates during the subsequent PB. This decrease appeared to be due mainly to the formation of clusters of low average Mg/Si ratio at 298 K that did not act as effective precursors to the development of elongated precipitates upon PB. The presence of these clusters lowered the matrix solute concentrations, and suppressed nucleation of more efficient (higher Mg/Si ratio) precursors of the elongated phases.

1. Introduction

Al–Mg–Si (6xxx) alloys are considered to be the most promising candidates for light weight, heat-treatable, body-sheet materials for automobiles because of their strength, good formability, and corrosion resistance [1]. Remarkably little is known for certain about early-stage precipitation as a function of temperature despite the commercial importance of these alloys. The following general precipitation sequence in Al–Mg–Si alloys has been suggested [2–6]:

$$\begin{aligned}&\text{SSSS} \rightarrow (\text{Si and Mg clusters} \rightarrow)\text{Mg} + \text{Si co-clusters}\\&\quad \rightarrow \text{Guinier-Preston (GP) zones} \rightarrow \beta'' \rightarrow \beta' \rightarrow \beta\end{aligned}$$

with SSSS being the supersaturated solute solution. There is doubt regarding the role (and even the existence) of separate Si- and Mg-rich clusters at the very earliest stages of ageing. Co-clusters of Mg + Si are believed to be crucial to the early-stage formation of precipitates at elevated temperatures, and thus the development of mechanical properties during the manufacture of automobile body-sheets. However, little is known for certain about the composition and structure of the co-clusters due to difficulties in the analysis of these ultra-small particles. The most detailed results concerning clusters have been obtained by atom probe [7–21]. Note that findings in the literature by different authors vary and occasionally contradict each other. The conflicting results in literature are partly due to the limited statistical data of the reported atom probe experiments as well as the different investigated alloy compositions.

Ambiguity exists regarding the phase or phases formed after the co-clusters and before β''. Most authors describe a single species, namely GP zones (or initial-β'' or pre-β''), even though the precipitates vary in size, shape and probably composition before transforming into β''. A wide range of possible GP zone structures has been proposed largely based on first-principle calculations [2,5,6,22–26]. However, no consensus exists regarding which structure is energetically most stable.

The needle-shaped β'' phase is only formed at elevated temperatures (>398 K [25]) and is seen as the main hardening phase for ternary Al–Mg–Si alloys. However, finishing heat treatments used in industry are too short to reach peak hardness in a single step. After stamping and painting, the final process step at a temperature of 433–453 K is only 20–30 min long as this is the time needed to cure the paint, hence the name paint-bake (PB) cycle. After this

---

* Corresponding author at: Lux Research Inc., 100 Franklin Street, 8th Floor, Boston, MA 02110, United States.

E-mail address: mathijsz@gmail.com (M.W. Zandbergen).

http://dx.doi.org/10.1016/j.actamat.2015.08.017

Please cite this article in press as: M.W. Zandbergen et al., Acta Mater. (2015), http://dx.doi.org/10.1016/j.actamat.2015.08.017

PB treatment the material should be high enough in strength to meet the automobile manufacturer's standards. Consequently, heat treatments given prior to the PB need to be finely tuned to obtain optimal PB hardening.

The aim of this paper is to establish which phases are present at different temperatures and to explore possible mechanisms by which they are formed. Three ageing temperatures of 298, 353 and 453 K are examined. The chosen heat treatment temperatures correspond closely to those used in engineering practise. Ageing at room temperature, also known as natural ageing (NA) imitates conditions during storage of the sheets. NA delays the age-hardening response during the following PB cycle by 20–30 min, effectively preventing any significant hardening during the PB [27,28]. In industry, steps are taken to reduce the effect of natural ageing. The heat treatment at 353 K mimics a commonly used step known as pre-ageing (PA), which mitigates the deleterious influence of NA [27]. Ageing at 453 K corresponds to the final PB heat treatment to cure the paint on body-sheets.

Recently, with the development of a new generation of APT instruments, it has become possible to obtain much more extensive atom probe datasets than previously. In the present work, precipitation in an Al–Mg–Si alloy has been revisited. Current-generation APT analysis and hardness measurements have been combined to determine the influence of ageing temperature on the precipitation sequence. Large APT datasets have been acquired under carefully controlled experimental conditions. This approach leads to greatly enhanced, statistically viable information, thus removing one of the major limitations of previous atom probe studies. The present paper reports the results of single and multi-stage ageing treatments on ternary Al–Mg–Si alloys. In an accompanying paper (Part II) we report on the effects of additions of copper to the base alloy [29].

2. Experimental

Full details on the experimental techniques, data interpretation methods and statistical analysis procedures can be found in the *Data in Brief* [30].

Table 1 shows the composition of the investigated ternary Al–Mg–Si alloy. Sheets were cold-rolled to 1 mm thickness. An overview of the heat treatments is given in Table 2. All heat treatments were performed in an air furnace unless stated otherwise. The samples were solid solution heat-treated (SSHT) at 835 K for 30 min followed by a water quench to room temperature. PB or PA treatments were commenced 1 or 3 min after the water quench, respectively. If necessary, the material was stored in liquid nitrogen after heat treatments to inhibit the influence of any subsequent NA. In some cases a thermal spike for 10 s at 453 K (referred to simply as a spike from now on) was given to investigate its effect on PA.

A calibrated Vickers indenter was used for hardness measurements. For APT analysis, two different types of 3D atom probe were used, a local-electrode atom probe (LEAP™) [31,32] and a large-angle-reflectron 3D atom probe (LAR-3DAP™) [33]. Analyses were carried out at specimen temperatures of 25–30 K and pulse voltages of 15–20% of the standing DC voltage. Needle-shaped specimens for APT experiments were made by a standard electropolishing method [34] from heat-treated thin bars. Transmission electron microscopy (TEM) was performed on a needle-shaped APT sample after 580 h PB using a FEI Tecnai microscope at TU Delft.

Table 2
Summary of heat treatments studied.

Heat treatment[a]	Results section
1 min NA + PB	3.1.2
NA	3.1.3
PA	3.1.4
NA + PB	3.2.1
PA + 1 week NA + PB	3.2.2
Spike + PA + NA (+PB)	3.2.3

[a] NA = natural ageing at 298 K, PA = pre-ageing at 353 K, PB = paint-bake at 453 K, Spike = 10 s at 453 K.

The total numbers of ions collected for a sample by APT ranged from 5 to 30 $\times$ 10^6 detected ions, and the numbers of particles examined in the early stages of ageing were typically between 100 and 500 per sample. The APT data were analysed using particle selection software in PoSAP™ and IVAS™. The particles were shown in 3D atom maps, in which only the Mg and Si atoms were depicted. The software used a Maximum Separation Method [34,35] for particle selection based on a nearest neighbour technique as described elsewhere [36]. For LEAP measurements, a separation distance (d) of 0.65 nm and N_{min} of 10 solute atoms was used. As N_{min} was set at 10, particles containing fewer than 10 detected solute atoms were not selected. A d of 0.70 nm was allowed for LAR-3DAP measurements. In some cases, further particle analysis was carried out using a N_{min} of 5 to estimate the number density for particles consisting of more than 5 solute atoms. The dimensions of each particle measured along three orthogonal axes were determined in IVAS™. The precipitate length corresponded to the longest axis. The shortest axis was used to indicate the diameter of particles that were needle-shaped.

It should be noted that LEAP and LAR-3DAP measurements can give differences in results with respect to particle chemistry and number density, especially in the cases of the very smallest particles. This is mainly due to differences in detection efficiency (see *Data in Brief* article, Ref. [30]). In general, the particle chemistries and number densities reported here are those detected by LEAP, to ensure full compatibility between data sets. In addition, comparison of number densities of small particles was only performed for measurements at similar low voltages (below 6 kV and within a 1 kV range). It should be noted that the presence of large elongated particles (>15 nm) after prolonged PB leads to failure in the detection of multiple ions evaporating per pulse from these larger precipitates [37–39]. Relatively more Si atoms were undetected than Mg atoms, thereby overestimating the average Mg/Si ratios of large elongated particles by 20–40%. In the Results section, only the unadjusted particle Mg/Si ratios as measured by APT are given. It should also be noted that local aberration effects exist due to ion trajectory differences between different phases [34] increase the apparently-measured width of the interface between matrix and precipitates by 2–3 nm. Only the detected widths are given in the Results section.

Table 1
Nominal and average measured composition of the alloy in wt% and at.%.

	Al	Si	Mg	Cu	Fe	Mn
(wt.%)	Balance	0.98 ± 0.02	0.46 ± 0.01	0.029 ± 0.002	0.17 ± 0.01	0.10 ± 0.02
(at.%)	Balance	0.94 ± 0.02	0.51 ± 0.01	0.013 ± 0.001	0.08 ± 0.01	0.05 ± 0.01
Measured by APT						
(at.%)	Balance	0.95 ± 0.01	0.46 ± 0.01	0.016 ± 0.001	–	0.03 ± 0.01

Please cite this article in press as: M.W. Zandbergen et al., Acta Mater. (2015), http://dx.doi.org/10.1016/j.actamat.2015.08.017